

---

# Phosphomolybdic acid-responsive Pickering emulsions stabilized by ionic liquid functionalized Janus nanosheets

Qing Bo Meng<sup>a</sup>, Peng Yang<sup>a</sup>, Tianyang Feng<sup>a</sup>, Xuyang Ji<sup>a,b</sup>, Qian Zhang<sup>a</sup>, Daliang Liu<sup>a</sup>, Shuyao Wu<sup>a</sup>, Fuxin Liang<sup>b\*</sup>, Zhaoliang Zheng<sup>c</sup> and Xi-Ming Song<sup>a\*</sup>

<sup>a</sup>Liaoning Key Laboratory for Green Synthesis and Preparative Chemistry of Advanced Materials, College of Chemistry, Liaoning University, Shenyang 110036, China.

E-mail: songlab@lnu.edu.cn; Fax: +86-24-62202380; Tel: +86-24-62202378

<sup>b</sup>State Key Laboratory of Polymer Physics and Chemistry, Institute of Chemistry, Chinese Academy of Sciences, Beijing 100190, China.

E-mail: liangfuxin@iccas.ac; Fax: +86-10-62559373; Tel: +86-10-82619206

<sup>c</sup>Stephenson Institute for Renewable Energy, Department of Chemistry, University of Liverpool, Liverpool, Crown Street, Liverpool, L69 7ZD, United Kingdom

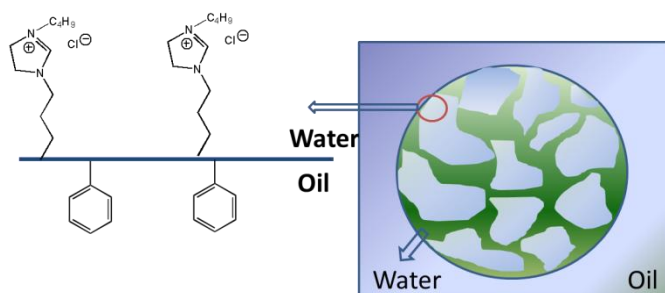
## Abstract

A type of ionic liquid functionalized high-aspect-ratio Janus SiO<sub>2</sub> nanosheets (IL-Janus nanosheets), which possesses a side terminated by imidazolin salt groups and the opposite side terminated by phenyl groups, was prepared and its emulsification performance was investigated. The surface wettability of ionic liquid functionalized side could be tailored via simple anion exchanging, giving the amphiphilic or totally hydrophobic Janus nanosheets. The influence of several parameters including surface wettability, particle concentration, oil composition, oil-water ratio as well as initial location of the nanosheets on the stability, morphology and type of the Pickering emulsions (O/W or W/O) stabilized by the amphiphilic IL-Janus nanosheets was evaluated. The research results revealed that average

---

emulsion droplets size was decreased with increase of nanosheets concentration below a concentration value but had almost no change beyond the concentration; catastrophic phase inversion phenomenon occurred by varying volume fraction of water phase in the oil-water systems, and transitional phase inversion could be achieved by in-situ exchanging  $\text{Cl}^-$  anion of the IL-Janus nanosheets with phosphomolybdate  $\text{H}_2\text{PMo}_{12}\text{O}_{40}^-$ . The responsiveness of Pickering emulsions towards phosphomolybdic acid is resulted from irreversible anion exchanging of  $\text{Cl}^-$  by  $\text{H}_2\text{PMo}_{12}\text{O}_{40}^-$  and the variation of surface wettability of the nanosheets.

**Keywords:** Janus nanosheet; Pickering emulsion; Ionic liquids; Phase inversion; Phosphomolybdic acid



Scheme 1. Schematic structure of IL-Janus nanosheets and formation of Pickering emulsions.

---

## 1. Introduction

Solid particles stabilized emulsions, which are usually mentioned as “Pickering emulsions”, have attracted much attention during the last decades, as many drawbacks of emulsions stabilized by conventional surfactants could be avoided [1-3]. Numerous studies based on Pickering emulsifiers have been reported, and revealed that their intrinsic features such as particle sizes and shapes, particle surface wettability[3], and experimental parameters such as particle concentration, initial location of emulsifiers[4] as well as volume ratio of the immiscible fluids have great influence on properties of the corresponding emulsions including stability, emulsion type, average emulsion droplets size and phase inversion behaviour[4-7]. One of the fundamental requirements for an ideal Pickering emulsifier is suitable surface wettability, which is also mentioned as “amphiphilicity”[8]. Generally, the so-called “amphiphilic” particles could be conceptually divided into two categories, one is the traditional choice where the “amphiphilic” particles possess homogeneous surface that could be partially wetted by both water and oil[3] while another one is the particles with separated hydrophilic and hydrophobic parts, which could be categorized as Janus materials[8]. The traditional choice means that the solid particles with extreme hydrophilic or hydrophobic surface could not be an ideal Pickering emulsifier, as they exhibit affinity only towards water or oil, respectively. On the other hand, Janus materials with compartmentalized hydrophilicity and hydrophobicity in its different parts are expected to be even thermodynamically stable at interface of immiscible liquids, owing to their amphiphilic properties similar to conventional surfactant, which is different from that of typical particle emulsifiers with homogeneous surface[9].

Binks and co-workers calculated that the desorption energy of Janus spherical particles at oil-water interface may be increased three times after maximizing the amphiphilicity of homogeneous particles[10], and the conclusion was experimentally verified by Glaser and co-workers afterwards[11]. Encouraged by the proved advantages of Janus particles as Pickering emulsifier, Janus materials with various

---

shape including spherical particles[12], cylinders[13], nanosheets[14], discs[15], snowman-like particles[16], flower-like particles[17], mushroom-like particles[18], etc. have been developed as Pickering emulsifier, and several researchers revealed that Janus nanosheets with high aspect ratio have their special superiority in the aspect of improving stability of emulsions[19-22]. The advantage of nanosheets-shaped Pickering particles should be mainly attributed to their restricted rotation [23, 24] and tendency of kinetically trapping[25] at the oil-water interface.

Recently, a novel kind of ionic liquid functionalized Janus SiO<sub>2</sub> nanosheets (IL-Janus nanosheets), with a side terminated by imidazolin salt groups and the opposite side terminated by phenyl groups, was successfully prepared by us[26] via interfacial materialization and subsequent ionization, which are massively producible with low cost and high reproducibility, compared with Janus materials prepared via other techniques such as phase separation, toposelective surface modification, microfluids, etc[22], and the emulsification capacity of the IL-Janus nanosheets and anion triggered de-emulsification was confirmed. The structure of IL-Janus nanosheets and the Pickering emulsions stabilized by them were shown in Scheme 1. It has been reported that surface wettability of the imidazolin salt terminated side could be manipulated by simple anion exchange[26, 27], while emulsion type (W/O or O/W) is theoretically determined by the surface wettability of solid particles according to Finkle's rule[28]. Therefore, the emulsion type should be influenced by different counter anions of IL-Janus nanosheets, and the corresponding responsive emulsions could be hopefully fabricated accordingly. Actually, de-emulsification of IL-Janus nanosheets stabilized Pickering emulsions is relatively easy to be achieved by exchanging hydrophilic anion with hydrophobic one[26], whereas phase inversion triggered by anions is much more difficult, because fine tuning of hydrophilicity of the hydrophilic anions is required. And also in view of that functional materials are easier to grow within the ionic liquids by specific interactions [29-34], the emulsions stabilized by the IL-Janus nanosheets could combine the features of ionic liquid functionalized materials, Janus materials as well as Pickering emulsion, giving a novel smart system for many applications including interfacial or biphasic catalysis,

---

control release system, etc., and it is hence necessary to systematically investigate the emulsification performances of IL-Janus nanosheets, and then develop novel anion responsive Pickering emulsions.

In the present study, stability, morphology and phase inversion behaviour of the IL-Janus nanosheets stabilized Pickering emulsions were investigated. The influence of the IL-Janus nanosheets concentration on the morphology of emulsions droplets was discussed in detail. Phase inversion behaviour of the emulsions was investigated by changing various factors including specie of counter anion, initial location of the nanosheets as well as oil-water ratio, and phosphomolybdic acid responsive emulsions were consequently developed.

## **2. Experimental**

### *2.1. Materials*

Triethoxy-3-(2-imidazolin-1-yl) propylsilane (IZPES) was purchased from Sigma-Aldrich. Phenyl-triethoxysilane (PTES) was purchased from Alfa Aesar. Tetraethyl orthosilicate (TEOS), 1-chlorobutane, potassium hexafluorophosphate (KPF<sub>6</sub>), silicotungstic acid hydrate (H<sub>4</sub>SiW<sub>12</sub>O<sub>40</sub>), phosphomolybdic acid hydrate (H<sub>3</sub>PMo<sub>12</sub>O<sub>40</sub>), paraffin (T<sub>m</sub>: 52-54 °C), ethanol, tetrahydrofuran (THF), n-octane, n-hexane, n-decane, n-heptane, n-dodecane, toluene were purchased from Sinopharm Chemical Reagent Co.. Hydrolyzed styrene–maleic anhydride (HSMA) copolymer was synthesized according to reference[35]. All of the reagents were used as received without further purification.

### *2.2. Preparation of the IL-Janus nanosheets*

The IL-Janus nanosheets was fabricated according to the reported procedure[26]. Briefly, 15 mL HSMA solution (10 wt.-%) was diluted with 75 mL distilled water, followed by adjusting pH to 2.5 with 2.0 M hydrochloride acid. The prepared solution was heated to 70 °C for use as water phase. On the other hand, an oil phase was produced by dissolving 5.2 g TEOS、 1.37 g IZPES、 1.2 g PTES in 25 g paraffin

---

(m.p.= 50-52 °C) which was melted under 70 °C in advance. The oil phase containing the silane precursors was mixed together with the water phase and emulsified by homogenizer under 12,000 rpm for 5 min to form O/W emulsion. A Sol-Gel process was performed at 70 °C for 12 h. After naturally cooled down to room temperature, the paraffin@silica core-shell microspheres were separated by suction filtration and washed with water. Finally, the paraffin core in the microspheres was removed by tetrahydrofuran (THF) with assist of ultrasonication, and the obtained imidazolin-based Janus hollow microspheres were consequently isolated by suction filtration and then rinsed with THF. The Janus hollow microspheres were dispersed in distilled water and then crushed by colloid milling for 15 min. After several centrifugation/redispersion cycles in ethanol and deionized water, the imidazolin-based Janus nanosheets were obtained.

0.1 g as-made imidazolin-based Janus nanosheets were allowed to disperse in 40 mL toluene with assist of ultrasonication followed by addition of 1.0 mL 1-chlorobutane and then refluxed for 24 h. Yellow powdered IL-Janus nanosheets with chloride ion as counter anion (Cl-based IL-Janus nanosheets) were produced after washing with toluene for several times as well as vacuum dried process.

### *2.3. Anion exchange of the IL-Janus nanosheets*

0.05 g Cl-based IL-Janus nanosheets were allowed to disperse in 25 mL distilled water with assist of ultrasonication followed by addition of 0.1 g (c.a. 0.543 mmol)  $\text{KPF}_6$  (potassium hexafluorophosphate) and then stirred at room temperature for 2 h. The precipitated white powdered  $\text{PF}_6$ -based IL-Janus nanosheets were isolated and then washed with distilled water for several times followed by vacuum dried process. Phosphomolybdic acid- and tungstosilicic acid-based IL-Janus nanosheets were also prepared via the same procedure except for using 0.991 g phosphomolybdic acid (c.a. 0.543 mmol) or 1.563 g tungstosilicic acid (c.a. 0.543 mmol) in place of  $\text{KPF}_6$ .

### *2.4. Fabrication of IL-Janus nanosheets stabilized emulsions*

---

The IL-Janus nanosheets fabricated by the above mentioned methodology were used to prepare Pickering emulsions. The total volume of oil phase and water phase was fixed as 2.0 mL, and the emulsions were fabricated by vigorous hand-shaking. An aqueous solution containing a trace amount of methyl orange as chromogenic agent was dropped into the water phase for better observation. The other experimental conditions such as composition of oil phase, concentration and initial location of the Janus nanosheets as well as oil-water ratio were varied in order to investigate their influence on the properties of fabricated emulsions.

### 2.5. Characterization

Fourier transform infrared spectroscopy (FT-IR) spectra of potassium bromide powder-pressed pellets were recorded on a Perkin-Elmer Spectrum one FT-IR spectrometer (Perkin-Elmer Corp., USA). Morphologies of the Janus particles and emulsion droplets were characterized with scanning electron microscopy (Hitachi SU-8010 at 10 KV) equipped with an energy dispersive X-ray (EDX) analyzer (Hitachi S-4300) and Nikon Eclipse Ti inverse optical microscope, respectively. The optical microscope was equipped with 4×, 10×, 20×, extra-long working distance 40×, and oil-immersion 100× Nikon objectives. The images of IL-Janus nanosheets stabilized emulsions were captured with a Lumenera Infinity X CCD camera. To enable visualization, emulsion samples were diluted by their continuous phase and then gently placed on microscope slides, which were capped with a closed glass cylinder to prevent evaporation.

### 2.6. Droplet Size Measurements

For each emulsion, up to 50 droplets were measured with Nano Measure software to determine their surface-weighted average droplet size  $D$ , which is defined as

$$D = \frac{\sum_i n_i D_i^3}{\sum_i n_i D_i^2} \quad (1)$$

where,  $n_i$  is the number of droplets with size  $D_i$ .

---

### 3. Results and discussion

#### 3.1. Synthesis of IL-Janus nanosheets

IL-Janus nanosheets were prepared through ionization of the imidazolin terminated nanosheets precursor according to our previous publication[26]. The precursor was fabricated by crushing treatment of the corresponding Janus hollow spheres, which were prepared via interfacial materialization of several types of silane agents including IZPES, PTES and TEOS at the liquid-liquid interface of the paraffin-in-water emulsion, followed by removal of the paraffin core. During the self-assembly and Sol-Gel process for the formation of paraffin@SiO<sub>2</sub> microspheres, PTES with hydrophobic phenyl groups and IZPES with hydrophilic imidazolin groups were located at the oil-water interface towards inner paraffin phase and outer aqueous phase, respectively. SEM image in Fig. S1 (left) showed that the prepared paraffin@SiO<sub>2</sub> microspheres had homogeneous smooth surfaces and their exterior diameters were in the range of 3-4 μm. After removing the paraffin templates by washing with THF, the imidazolin-terminated hollow silica spheres were formed as shown in Fig. S1 (right), where the observed wrinkled surfaces indicated that the hollow spheres were collapsed to some degree, while its shell structure was still preserved. The imidazolin-based Janus nanosheets before (a) and after (b) ionization were characterized by FT-IR spectra and shown in Fig. S2. The peaks located at 1,660, 2,942, 1,080 cm<sup>-1</sup> are attributed to vibration of C=N bond, stretching of C-H bond and Si-O-Si bond, respectively. Aromatic out-of-plane bending vibrations of phenyl groups are connected to the peaks located in 700-900 cm<sup>-1</sup>. The presence of Cl element in EDX spectra of the ionic liquid functionalized Janus nanosheets (Fig. S3B) proved the success of ionization, compared to EDX spectra of the imidazolin based one (Fig. S3A). SEM images of the imidazolin-based Janus nanosheets (Fig. S3C) and IL-Janus nanosheets (Fig. S3D) showed no significant variation of the morphology after the ionization.

---

Counter anion  $\text{Cl}^-$  of the Cl-based IL-Janus nanosheets was exchanged with  $\text{PF}_6^-$ ,  $\text{H}_2\text{PMo}_{12}\text{O}_{40}^-$  and  $\text{H}_3\text{SiW}_{12}\text{O}_{40}^-$ , respectively, so as to investigate the influence of counter anion on emulsification performance of the nanosheets. FT-IR spectra of the IL-Janus nanosheets with different counter ions including  $\text{Cl}^-$ ,  $\text{PF}_6^-$ ,  $\text{H}_2\text{PMo}_{12}\text{O}_{40}^-$  and  $\text{H}_3\text{SiW}_{12}\text{O}_{40}^-$  were summarized in Fig. S4. All of the feature peaks of imidazolin-based Janus nanosheets were still remained in the ionized materials. The peak located at  $845\text{ cm}^{-1}$  due to stretching vibration of P-F bond was observed in curve b, proving the successful replacement of  $\text{Cl}^-$  with  $\text{PF}_6^-$ , while the peaks located at  $947$  (Mo=O stretching vibration),  $907$  (Mo-O-Mo asymmetric stretching vibration) and  $802\text{ cm}^{-1}$  (stretching vibrations of the bridging Mo-O-Mo groups) shown in curve c could support the existence of  $\text{H}_2\text{PMo}_{12}\text{O}_{40}^-$  anion. The success of anion exchange by  $\text{H}_3\text{SiW}_{12}\text{O}_{40}^-$  was also verified by the appearance of new peaks located at  $970$  (symmetric vibration of W=O),  $924$  (asymmetric vibration of W=O) and  $803\text{ cm}^{-1}$  (vibration of W-O-W) as shown in curve d, compared to that of Cl-based IL-Janus nanosheets in curve a.

### *3.2. Emulsification performance of IL Janus nanosheets*

#### *3.2.1. Influence of the amphiphilicity of Janus nanosheets on its emulsification performance*

Amphiphilicity of particles is one of the most fundamental requirements as an ideal Pickering emulsifier, whereas surfactant-like amphiphilicity of solid particles could be realized in Janus structure. The immobilization of ionic liquid functional groups onto the Janus nanosheets can endow it with in-situ controllable amphiphilicity. It is widely known that quaternization of N atom in imidazolin group could significantly increase its hydrophilicity and  $\text{PF}_6^-$  is capable of endowing ionic liquid functionalized surface with hydrophobicity. And therefore imidazolin-, Cl and  $\text{PF}_6^-$  based Janus nanosheets, which have weak hydrophilicity, strong hydrophilicity and hydrophobicity on the imidazolin functionalized side, respectively, were used as Pickering emulsifier for the various binary system of water-oil (toluene, n-hexane,

---

n-octane, n-decane and n-dodecane) to systematically investigate the influence of amphiphilicity of the Janus nanosheets on their emulsification performance.

The results of emulsifying experiments revealed that the PF<sub>6</sub>-based IL-Janus nanosheets exhibited no emulsifying capacity as reported in our previous publication[26]. Photographs of the oil-water emulsions with various types of oil stabilized by imidazolin- and Cl-based Janus nanosheets after standing for 30 d are shown in Fig. 1. The existence of emulsified phase (upper) in Fig. 1a indicated that Cl-based IL-Janus nanosheet is a widely applicable Pickering emulsion stabilizer. On the other hand, the photographs in Fig. 1b indicated that the emulsification capability of imidazolin-based Janus nanosheets was unsatisfactory irrespective of oil composition, as de-emulsification happened within a short time scale. The significant difference of emulsifying capacity of the three Janus nanosheets should be attributed to their varied amphiphilicity.

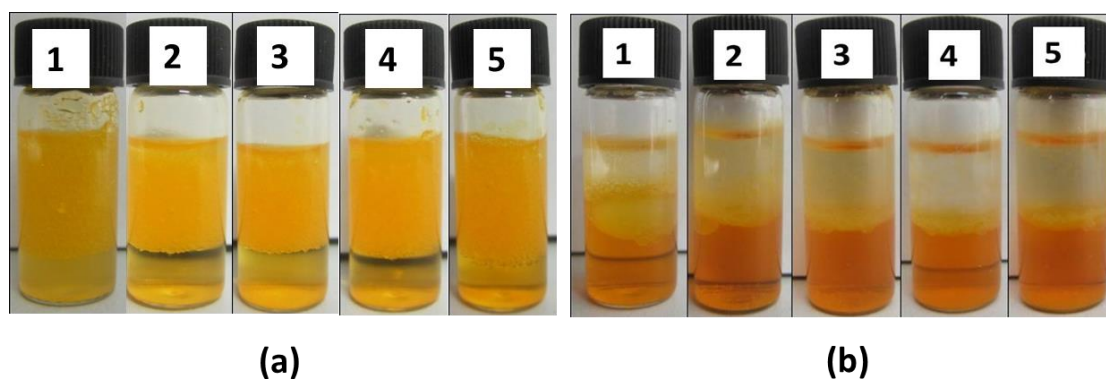


Fig. 1. Photographs of mixture of water (1.0 mL) and organic solvents (1: toluene; 2: n-hexane; 3: n-octane; 4: n-decane; 5: n-dodecane; 1.0 mL) emulsified by 2 mg Cl-based IL-Janus nanosheets (a) and 2 mg imidazolin-based Janus nanosheets (b) after standing for 30 d.

### 3.2.2. Influence of the IL-Janus nanosheets concentration on the morphology of emulsions droplets

Herein, “morphology” means size and shape of emulsion droplets. Concentration of emulsifier in a Pickering emulsion is an important influencing factor on average emulsion droplets size. The emulsion droplets size determines the oil-water interface

---

area of emulsion, which is important for various applications of emulsions (e.g. interfacial or biphasic catalysis).

A serial of Pickering emulsions stabilized by various concentrations of the Cl-based IL-Janus nanosheets were prepared and their photographs were collected in Fig. 2. All of the emulsion droplets are visible to naked eyes, especially for those with lower concentrations of Janus nanosheets (No. 1-6 in Fig. 2), and the emulsion droplets size was continuously decreased from millimeter scale to micrometer scale with increase of Janus nanosheets concentration. The relatively larger droplets of emulsions in No.1-3 of Fig. 2 have irregular shapes due to higher flowability of the large internal oil droplets. The creaming phenomenon was observed in all of the emulsion systems of Fig. 2, but volume fraction of the emulsified phase was gradually increased with increase of the emulsifier concentration for these emulsion systems, which are in accordance with the results reported by other researchers[36].

The emulsions No.7-12 with relatively smaller droplets size in Fig. 2 were characterized by optical microscope as shown in Fig. 3. Irregular shapes of droplets were also observed for the emulsions No. 4-6 in Fig. 3. The phenomenon could be explained by aggregation of over saturated nanosheets[37] and increased viscosity of continuous phase[38], which will be further discussed in detail in the following paragraphs.

Based on the theory of limited coalescence[5], Folter and co-workers derived expression relating the droplet size to the amount and size of adsorbed solid particles and the volume of the dispersed phase for cubic shaped particles stabilized Pickering emulsions, as shown in equation (2)[6], where,  $D$  is the average droplets size of emulsions,  $d$  is the average edge size of the cubic Pickering particles,  $p$  is the density of Pickering particles,  $V_{oil}$  is the volume of oil phase,  $C$  is the interface coverage and  $m_p^{tot}$  is the total mass of Pickering particles.

$$D = \frac{6d\rho_p V_{oil}C}{m_p^{tot}} \quad (2)$$

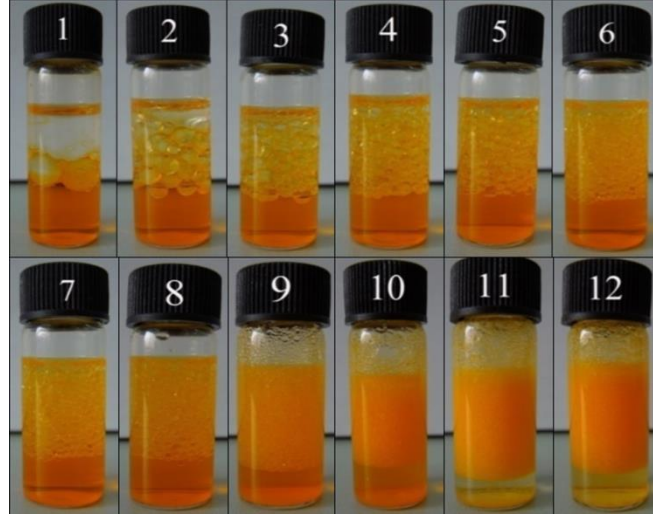


Fig. 2. Photographs of toluene (1.0 mL) /water (1.0 mL) emulsions stabilized by various amount of the CI-based IL-Janus nanosheets (1: 0.13, 2: 0.28, 3: 0.38, 4: 0.44, 5: 0.52, 6: 0.64, 7: 0.73, 8: 0.84, 9: 2.18, 10: 4.63, 11: 8.73, 12: 12.94 mg) after standing for 30 d.

However, equation (2) is not suitable for the nanosheets-shaped Pickering emulsifiers used in the present study. In order to deduce the equation for nanosheets based Pickering emulsion systems, the following assumptions are necessary: (i) both the emulsion droplets and the nanosheets were uniform in size; (ii) the emulsion droplets and the nanosheets are spherical and rectangular sheet in shape, respectively; (iii) all of the added Janus nanosheets were uniformly adsorbed on the oil-water interface and packaged into monolayer before full coverage; (iv) the interfacial curvature was ignored, and the flat nanosheets were hence supposed to be perfectly adsorbed onto spherical emulsion droplets.

Based on the above assumptions, the total oil-water interfacial area of the emulsion droplets  $A_{int}$  is given by:

$$A_{int} = N_d \pi D^2 = \frac{V_{oil}}{\frac{1}{6}\pi D^3} \cdot \pi D^2 = \frac{6V_{oil}}{D} \quad (3)$$

where  $N_d$  is the number of emulsion droplets (the average droplet size is assumed to be  $D$ ). While the total interfacial area  $A_p^{tot}$  occupied by the Janus nanosheets is given by:

$$A_p^{tot} = N_p A_p = N_p l m = \frac{m_p^{tot}}{\rho_p l m h} \cdot l m = \frac{m_p^{tot}}{\rho_p h} \quad (4)$$

where  $N_p$  represents the number of particles adsorbed at the interface,  $A_p$  is the interface area occupied by each particle,  $l$ ,  $m$  and  $h$  are length, width and thickness of the nanosheets, respectively. Herein, interface coverage  $C$  is defined by fraction of the interface area covered by the nanosheets:

$$C = \frac{A_p^{tot}}{A_{int}} = \frac{m_p^{tot} D}{6V_{oil} \rho_p h} \quad (5)$$

The relationship between amount of the nanosheets and the average emulsion droplets size could be written as:

$$D = \frac{6h\rho_p V_{oil} C}{m_p^{tot}} \quad (6)$$

The difference between equation (2) and (6) is that edge size  $d$  in the equation (2) was replaced by thickness  $h$  in the present study, and equation (2) is a special case of equation (6). According to equation (6), the interface coverage  $C$  is inversely proportional to the thickness  $h$  at a fixed emulsification condition.

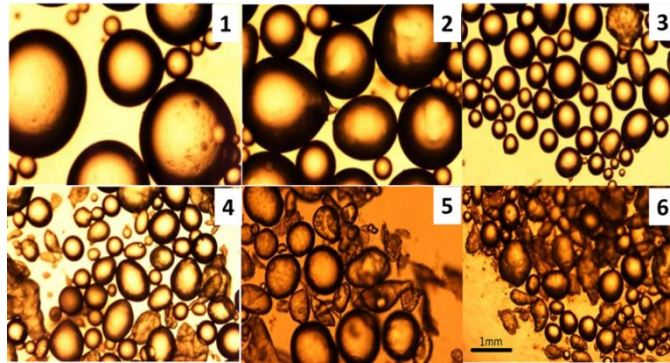


Fig. 3. Optical microscope photographs of toluene (1.0 mL) /water (1.0 mL) emulsion stabilized by various amount of Cl-based IL-Janus nanosheets (1: 0.73, 2: 0.84, 3: 2.18, 4: 4.63, 5: 8.73, 6: 12.94 mg) after standing for 30 d.

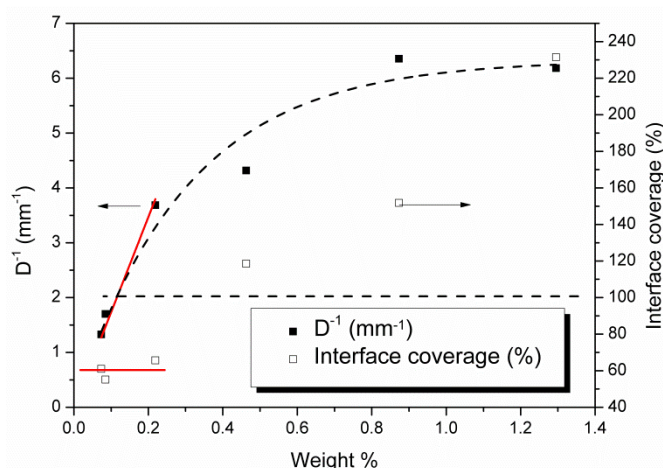


Fig. 4. Relationship between inverse average emulsion droplet size ( $D^{-1}$ ) and concentration of the Cl-based IL-Janus nanosheets (closed squares) and relationship between estimated interface coverage and concentration of the nanosheets (open squares), in toluene (1.0 mL) /water (1.0 mL) emulsion.

The inverse average emulsion droplet sizes ( $D^{-1}$ ) of the emulsions in Fig. 3 against the corresponding concentration of the IL-Janus nanosheets (wt. %, based on aqueous phase) were plotted in Fig. 4 (closed squares). The relationship of  $D^{-1}$  and the concentrations is linear within the initial concentration range (< c.a. 0.2 wt. %, emulsions No. 1-3 in Fig. 3). The linearship means that the interface coverage is a constant in the range of concentration according to equation (6). However, the relationship between inverse average emulsion droplets size ( $D^{-1}$ ) and concentration of IL-Janus nanosheets deviated from the above mentioned linearship in the range of concentration higher than c.a. 0.2 wt. % and the curve gradually approached to a plateau. The appearance of plateau in the range of concentration higher than c.a. 0.8 wt.% means that there is a minimum average droplets size in the present Pickering emulsion systems, which was also reported by other researchers[37]. The interface coverage could be calculated according to equation (5) by roughly assuming the density and thickness of silica-based Pickering particle as 2.32 g/cm $^3$ [39] and 65 nm[40], respectively, and the calculated values were shown in Fig. 4 (open squares). The calculated interface coverage in the range of concentration lower than c.a. 0.2 wt. %

---

was c.a. 60 %. In the range of concentration higher than c.a. 0.2 wt. %, the interface coverage was increased with increase of the nanosheets concentration, and the interface coverage was higher than 100 % in the range of concentration higher than 0.4 wt.%. The change of interface coverage should be due to that the excess of further added Janus nanosheets aggregated at the interface or dispersed in the continuous phase, which lead to increased viscosity of continuous phase, resulting in the irregular shape of emulsion droplets shown in No. 4-6 of Fig. 3.

### 3.2.3. Phase inversion behavior

Catastrophic phase inversion of Pickering type emulsions induced by increasing volume fraction of dispersed phase has been widely studied[36]. It has been revealed that the phase inversion position is mainly dependent on surface wettability of Pickering emulsifiers, which obeys the Finkle's rule, i.e., solid particles with relatively higher hydrophilicity are in favor of forming O/W type emulsion, and vice versa. In view of the amphiphilicity of IL-Janus nanosheets could be adjusted by anion exchange, the influence of different hydrophilic counter anions on the catastrophic phase inversion was investigated in the present work.

2 mg of Cl-based IL-Janus nanosheets were initially dispersed into various volume of water or oil phase, respectively, and then the other phase was added to keep the total volume to 2.0 mL. Volume fraction of the water phase was noted as  $\Phi_w$ , and the  $\Phi_w$  value at phase inversion position was noted as  $\Phi_{w,pi}$ . Photographs of the fabricated water-toluene emulsions are shown in Fig. 5. Catastrophic phase inversion phenomenon was observed in No. 9, 10 of Fig. 5a and No. 5, 6 of Fig. b, regardless of initial location of the Janus nanosheets. Optical microscope photograph of a typical emulsion at state closed to catastrophic phase inversion is shown in Fig. 6. Some multiple emulsion droplets and irregular shaped droplets were observed in Fig. 6, indicating that catastrophic phase inversion occurred through formation of multiple emulsion droplets and deformation of spherical shaped emulsion droplets[41]. The catastrophic phase inversion position in Fig. 5 was also varied by different initial location of the Pickering emulsifier. Concretely, the  $\Phi_{w,pi}$  was 0.495~0.500, when the

---

nanosheets initially dispersed in water, while the  $\Phi_{w,pi}$  shifted to 0.700~0.705 in the case of toluene as initial location. The difference in catastrophic phase inversion position was generally attributed to “hysteresis of contact angle” which is considered to be related to roughness of particle surface[36]. .

Heteropolyanions are a kind of anions with catalysis[42, 43], and the IL-Janus nanosheets with heteropolyanions are expected to be applied for emulsions based interfacial catalytic reactions. Our experimental results revealed that the phosphomolybdic acid-based IL-Janus nanosheets have good emulsification capability, while the tungstosilicic acid-based IL-Janus nanosheets failed to give stable emulsions. As shown in Fig. 7, catastrophic phase inversion and “hysteresis of contact angle” phenomenon were also observed for phosphomolybdic acid-based IL-Janus nanosheets stabilized emulsions. Interestingly, compared with the Cl-based IL-Janus nanosheets stabilized emulsions, the catastrophic phase inversion positions in Fig. 7 were shifted. Concretely, the emulsion type was switched from W/O to O/W at  $\Phi_{w,pi}$  =0.460~0.465 or  $\Phi_{w,pi}$  =0.620~0.625 in the case that water phase or oil phase was used as initial location, respectively. The two  $\Phi_{w,pi}$  values at phase inversion position, are lower than  $\Phi_{w,pi}$  of the Cl-based IL-Janus nanosheets fabricated emulsion systems. Decrease of the two  $\Phi_{w,pi}$  values was resulted from the varied surface wettability of the IL-Janus nanosheets due to anion exchange[27], i.e. the phosphomolybdic acid-based IL-Janus nanosheets exhibits higher hydrophilicity than Cl-based one.



Fig. 5. Photographs of water-toluene emulsions (2.0 mL) stabilized by 2.0 mg CI-based IL-Janus nanosheets with various volume fraction of water ( $\Phi_w$ ) after standing for 30 d.: a. water as initial location, No. 1-12:  $\Phi_w = 0.300, 0.400, 0.425, 0.450, 0.475, 0.480, 0.485, 0.490, 0.495, 0.500, 0.600$  and  $0.700$ , No.1-9: W/O type emulsions, No. 10-12: O/W type emulsions; b. toluene as initial location, No. 1-10:  $\Phi_w = 0.300, 0.400, 0.500, 0.600, 0.700, 0.705, 0.710, 0.715, 0.720$  and  $0.725$ , No.1-5: W/O type emulsions, No. 6-10: O/W type emulsions.

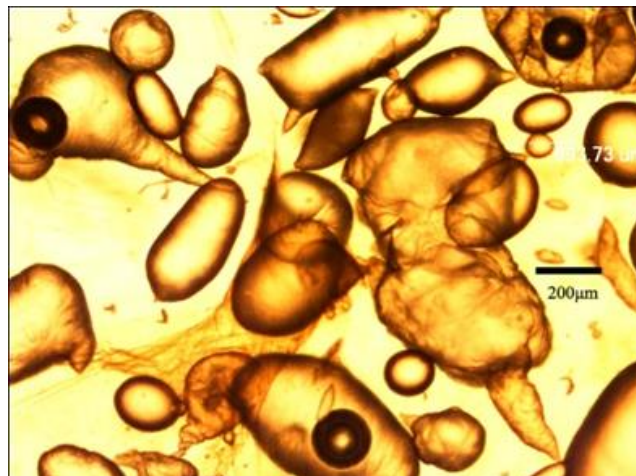


Fig. 6. Optical microscope photograph of the emulsion No. 9 in Fig. 5a at the position of catastrophic phase inversion.

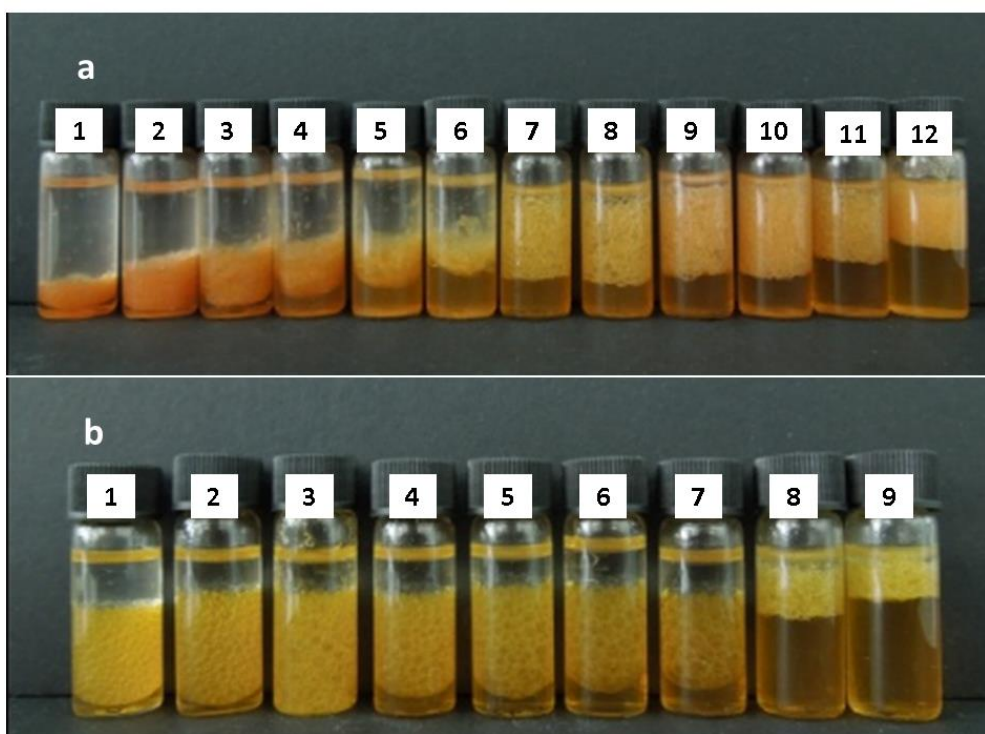


Fig. 7. Photographs of water-toluene emulsions (2.0 mL) stabilized by 2.0 mg phosphomolybdic acid-based IL-Janus nanosheets with various volume fraction of water ( $\Phi_w$ ) after standing for 30 d.: a. water as initial location, No. 1-12:  $\Phi_w = 0.200, 0.300, 0.400, 0.450, 0.455, 0.460, 0.465, 0.470, 0.475, 0.500, 0.600$  and  $0.700$ , No.1-6: W/O type emulsions, No. 7-12: O/W type emulsions; b. toluene as initial location, No. 1-9:  $\Phi_w = 0.300, 0.400, 0.500, 0.600, 0.610, 0.615, 0.620, 0.625$  and  $0.650$ , No.1-7: W/O type emulsions, No. 8-9: O/W type emulsions.

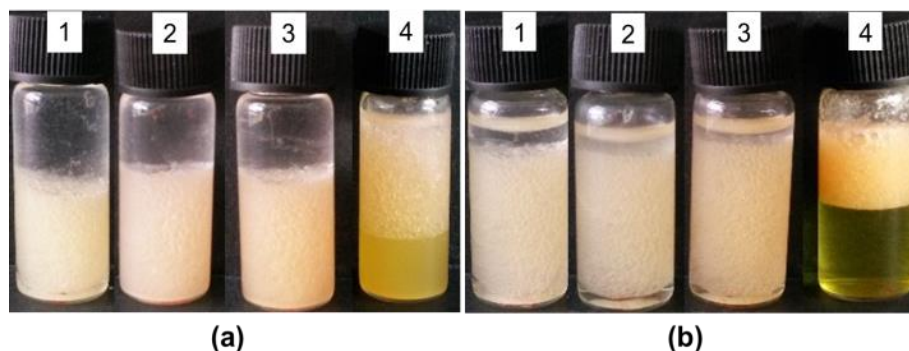


Fig. 8. Photographs of the toluene-water emulsions (No.1) with  $\Phi_w = 0.475$  (a) and  $0.660$  (b) stabilized by  $2.0$  mg Cl-based IL-Janus nanosheets, and the emulsions (No. 2-4) obtained by adding  $0.0025$ ,  $0.005$ ,  $0.01$  mmol of phosphomolybdic acid into No. 1. Water (a) and toluene (b) were used as the initial phase of the emulsifiers, respectively, and the total volume were fixed to be  $2.0$  mL for all the emulsion systems.

#### 3.2.4. Phosphomolybdic acid-responsiveness of the IL-Janus nanosheets stabilized emulsions

In addition to catastrophic phase inversion, Pickering emulsions could also be inverted by varying surface wettability of solid particles, which is defined as transitional phase inversion. The above results encouraged us to investigate whether an anion-responsive transitional phase inversion could be achieved by adding phosphomolybdic acid to the Cl-based IL-Janus nanosheets stabilized emulsion system. The corresponding experimental results were shown in Fig. 8. No phase inversion phenomenon was observed when less amount of phosphomolybdic acid added to the original W/O emulsions No. 1 of Fig. 8a and b, as shown in No. 2-3 of Fig. 8a and b regardless of the initial location, but when the amount increased to a fixed value, phase inversion occurred and O/W emulsions were formed as shown in No. 4 of Fig. 8a and b. This finding should be attributed to increase of hydrophilicity of the IL-Janus nanosheets after the anion exchanging, and is in accordance with the results obtained in the above mentioned study of catastrophic phase inversion, i.e., Cl-

---

and phosphomolybdic acid based IL-Janus nanosheets gave W/O and O/W type emulsions under the  $\Phi_w$  used in Fig. 8 (0.475 or 0.660 when water or toluene as initial phase), respectively. Considering that acidity of the water phase may have an influence on the transitional phase inversion, the acidity of water phase No. 1 of Fig. 8a and b was adjusted by adding 0.1 mmol hydrochloride acid aqueous solution to the emulsions, and the pH value of water phase in the emulsions were from 6 to 1 after the addition of HCl. Phase inversion phenomenon was not observed after the addition of HCl, even though the introduced amount of  $H^+$  is actually higher than that of No. 4 in Fig 8 (0.03 mmol), confirming that the phase inversion is only attributed to responsiveness of the emulsions towards phosphomolybdic acid. Further, the possibility of reversible phase inversion was investigated via addition of a sodium chloride aqueous solution into the emulsions stabilized by phosphomolybdic acid-based IL-Janus nanosheets (No.4 of Fig. 8a and b), and the results showed that the phase inversion phenomenon not happened as expected, regardless of added amount of chloride anion, which may be attributed to rather high interaction force between the imidazolium cations and  $H_2PMO_{12}O_{40}^-$  anions, hindering the anion exchange[44]. Actually the phosphomolybdic acid-based IL-Janus nanosheets could be obtained by addition of phosphomolybdic acid into Cl-based Janus nanosheets aqueous solution, i.e. replacing  $Cl^-$  with  $H_2PMO_{12}O_{40}^-$ , which has been confirmed by FT-IR spectra (Fig. S4), but the opposite pathway could not be realized for obtaining Cl-based ones. The results on water contact angle measurements in Fig. S5 proved that hydrophilicity of Cl-based IL functionalized surface was indeed enhanced after  $Cl^-$  was exchanged with  $H_2PMO_{12}O_{40}^-$ . Therefore, the phase inversion of emulsions stabilized by the Cl-based IL-Janus nanosheets, stimulated by addition of phosphomolybdic acid, was attributed to the irreversible anion exchanging and the variation of surface wettability. In addition, we tried to use other types of anions including  $BF_4^-$ ,  $NO_3^-$ ,  $HSO_4^-$ , etc. to achieve phase inversion of Cl-based IL-Janus nanosheets stabilized emulsions, but the phase inversion phenomenon was not observed. The reason should be that the  $BF_4^-$ ,  $NO_3^-$  and  $HSO_4^-$ -based IL-Janus nanosheets have similar hydrophilicity with Cl-based ones and the anion exchanging

---

was reversible. We have also studied the catastrophic phase inversion behaviour of emulsion stabilized by  $\text{BF}_4^-$ ,  $\text{NO}_3^-$  and  $\text{HSO}_4^-$ -based IL-Janus nanosheets, and all the phase inversion positions were not changed compared to that of  $\text{Cl}^-$ -based ones. The results proved that  $\text{BF}_4^-$ ,  $\text{NO}_3^-$  and  $\text{HSO}_4^-$ -based IL-Janus nanosheets have similar hydrophilicity to  $\text{Cl}^-$ -based ones, and thus the addition of  $\text{BF}_4^-$ ,  $\text{NO}_3^-$ ,  $\text{HSO}_4^-$  could not induce transitional phase inversion of  $\text{Cl}^-$ -based IL-Janus nanosheets stabilized emulsions.

Some responsive emulsions based on various types of stimuli such as pH,  $\text{CO}_2$ , temperature etc. have already been reported[45]. And in the present research, the phosphomolybdic acid-responsive phase inversion of Pickering emulsion systems was developed. To our best knowledge, no related study was reported yet. The novel phosphomolybdic acid-responsive emulsion system realized in present study is based on anion exchange of supported ionic liquids, where ionic liquids are a broad family of functional materials composed by numerous kinds of cations and anions. Therefore, the present research can provide a strategy for fabricating novel stimuli-responsive emulsions or other related materials, which have potential application on control-release process, oil recovery, anion sensing, emulsion polymerization, recovery of nano-particle catalysts, cosmetics, etc.[45, 46].

#### **4. Conclusions**

In this work, a kind of phosphomolybdic acid-responsive Pickering emulsions stabilized by the amphiphilic IL-Janus nanosheets was developed for the first time. We investigated the influence of surface wettability, particle concentration, oil composition, oil-water ratio as well as initial location of the nanosheets on the stability, morphology and emulsion types stabilized by the amphiphilic IL-Janus nanosheets. The research results revealed that the average emulsion droplets size of  $\text{Cl}^-$ -based IL-Janus nanosheets stabilized emulsions was decreased with increase of the nanosheets concentration below a concentration value but had almost no change beyond the concentration due to the self-aggregation of excess of nanosheets; catastrophic phase inversion phenomenon of the IL-Janus nanosheets stabilized

---

emulsions occurred via varying volume fraction of water phase, and transitional phase inversion could be achieved by in-situ exchanging counter anion  $\text{Cl}^-$  of the IL-Janus nanosheets by  $\text{H}_2\text{PMo}_{12}\text{O}_{40}^-$ . The responsiveness of Pickering emulsions towards phosphomolybdic acid is resulted from irreversible anion exchanging of  $\text{Cl}^-$  by  $\text{H}_2\text{PMo}_{12}\text{O}_{40}^-$  and the variation of surface wettability of the nanosheets. The results in the present study revealed that smart Pickering emulsions, which have potential application in various fields, e.g. designing interfacial catalysis system, and preparation of functional materials etc., could be constructed by the IL-Janus nanosheets.

## Acknowledgement

This work was supported by the National Natural Science Foundation of China [No. 51273087 and 51622308].

## References

- [1] E.S. Read, S. Fujii, J.I. Amalvy, D.P. Randall, S.P. Armes, Effect of varying the oil phase on the behavior of pH-responsive latex-based emulsifiers: Demulsification versus transitional phase inversion, *Langmuir* 20(18) (2004) 7422-7429.
- [2] T. Li, H. Liu, L. Zeng, W. Miao, Y. Wu, Study of emulsion polymerization stabilized by amphiphilic polymer nanoparticles, *Colloid. Polym. Sci.* 289(14) (2011) 1543-1551.
- [3] Y. Chevalier, M.-A. Bolzinger, Emulsions stabilized with solid nanoparticles: Pickering emulsions, *Colloids Surf., A* 439 (2013) 23-34.
- [4] B.P. Binks, J.A. Rodrigues, Types of phase inversion of silica particle stabilized emulsions containing triglyceride oil, *Langmuir* 19(12) (2003) 4905-4912.
- [5] S. Arditty, C.P. Whitby, B.P. Binks, V. Schmitt, F. Leal-Calderon, Some general features of limited coalescence in solid-stabilized emulsions, *Eur. Phys. J. E* 11(3) (2003) 273-281.
- [6] J.W.J. de Folter, E.M. Hutter, S.I.R. Castillo, K.E. Klop, A.P. Philipse, W.K. Kegel, Particle shape anisotropy in Pickering emulsions: Cubes and peanuts, *Langmuir* 30(4) (2014) 955-964.
- [7] N.P. Ashby, B.P. Binks, Pickering emulsions stabilised by Laponite clay particles, *Phys. Chem. Chem. Phys.* 2(24) (2000) 5640-5646.

- 
- [8] A. Kumar, B.J. Park, F. Tu, D. Lee, Amphiphilic Janus particles at fluid interfaces, *Soft Matter* 9(29) (2013) 6604-6617.
- [9] N. Ballard, S.A.F. Bon, Equilibrium orientations of non-spherical and chemically anisotropic particles at liquid–liquid interfaces and the effect on emulsion stability, *J. Colloid Interface Sci.* 448 (2015) 533-544.
- [10] B.P. Binks, P.D.I. Fletcher, Particles adsorbed at the oil–water interface: A theoretical comparison between spheres of uniform wettability and “Janus” particles, *Langmuir* 17(16) (2001) 4708-4710.
- [11] N. Glaser, D.J. Adams, A. Böker, G. Krausch, Janus particles at liquid–liquid interfaces, *Langmuir* 22(12) (2006) 5227-5229.
- [12] S. Jiang, M.J. Schultz, Q. Chen, J.S. Moore, S. Granick, Solvent-free synthesis of Janus colloidal particles, *Langmuir* 24(18) (2008) 10073-10077.
- [13] T.M. Ruhland, A.H. Gröschel, N. Ballard, T.S. Skelton, A. Walther, A.H.E. Müller, S.A.F. Bon, Influence of Janus particle shape on their interfacial behavior at liquid–liquid interfaces, *Langmuir* 29(5) (2013) 1388-1394.
- [14] H. Wu, W. Yi, Z. Chen, H. Wang, Q. Du, Janus graphene oxide nanosheets prepared via Pickering emulsion template, *Carbon* 93 (2015) 473-483.
- [15] R. Deng, F. Liang, P. Zhou, C. Zhang, X. Qu, Q. Wang, J. Li, J. Zhu, Z. Yang, Janus nanodisc of diblock copolymers, *Adv. Mater.* 26(26) (2014) 4469-4472.
- [16] Y. Sun, F. Liang, X. Qu, Q. Wang, Z. Yang, Robust reactive Janus composite particles of snowman shape, *Macromolecules* 48(8) (2015) 2715-2722.
- [17] W. Zhai, T. Li, Y.-F. He, Y. Xiong, R.-M. Wang, One-pot facile synthesis of half-cauliflower amphiphilic Janus particles with pH-switchable emulsifiabilities, *RSC Advances* 5(93) (2015) 76211-76215.
- [18] E. Passas-Lagos, F. Schüth, Amphiphilic Pickering emulsifiers based on mushroom-type Janus particles, *Langmuir* 31(28) (2015) 7749-7757.
- [19] B. Madivala, S. Vandebriel, J. Fransær, J. Vermant, Exploiting particle shape in solid stabilized emulsions, *Soft Matter* 5(8) (2009) 1717-1727.
- [20] J.S. Guevara, A.F. Mejia, M. Shuai, Y.-W. Chang, M.S. Mannan, Z. Cheng, Stabilization of Pickering foams by high-aspect-ratio nano-sheets, *Soft Matter* 9(4) (2013) 1327-1336.
- [21] A.F. Mejia, A. Diaz, S. Pallela, Y.-W. Chang, M. Simonetty, C. Carpenter, J.D. Batteas, M.S. Mannan, A. Clearfield, Z. Cheng, Pickering emulsions stabilized by amphiphilic nano-sheets, *Soft Matter* 8(40) (2012) 10245-10253.
- [22] J. Hu, S. Zhou, Y. Sun, X. Fang, L. Wu, Fabrication, properties and applications of Janus particles, *Chem. Soc. Rev.* 41(11) (2012) 4356-4378.
- [23] Y. Nonomura, S. Komura, K. Tsujii, Adsorption of microstructured particles at liquid–liquid interfaces, *J. Phys. Chem. B* 110(26) (2006) 13124-13129.
- [24] Y. Liu, F. Liang, Q. Wang, X. Qu, Z. Yang, Flexible responsive Janus nanosheets, *Chem. Commun.* 51(17) (2015) 3562-3565.
- [25] J. Kim, L.J. Cote, F. Kim, W. Yuan, K.R. Shull, J. Huang, Graphene oxide sheets at interfaces, *J. Am. Chem. Soc.* 132(23) (2010) 8180-8186.

- 
- [26] X. Ji, Q. Zhang, F. Liang, Q. Chen, X. Qu, C. Zhang, Q. Wang, J. Li, X. Song, Z. Yang, Ionic liquid functionalized Janus nanosheets, *Chem. Commun.* 50(43) (2014) 5706-5709.
- [27] B.S. Lee, Y.S. Chi, J.K. Lee, I.S. Choi, C.E. Song, S.K. Namgoong, S.-g. Lee, Imidazolium ion-terminated self-assembled monolayers on Au: Effects of counteranions on surface wettability, *J. Am. Chem. Soc.* 126(2) (2004) 480-481.
- [28] P. Finkle, H.D. Draper, J.H. Hildebrand, The theory of emulsification<sup>1</sup>, *J. Am. Chem. Soc.* 45(12) (1923) 2780-2788.
- [29] J. Dupont, R.F. de Souza, P.A.Z. Suarez, Ionic liquid (molten salt) phase organometallic catalysis, *Chem. Rev.* 102(10) (2002) 3667-3692.
- [30] P. Wasserscheid, W. Keim, Ionic liquids—new “solutions” for transition metal catalysis, *Angew. Chem. Int. Ed.* 39(21) (2000) 3772-3789.
- [31] R. Sheldon, Catalytic reactions in ionic liquids, *Chem. Commun.* (23) (2001) 2399-2407.
- [32] A.C. Cole, J.L. Jensen, I. Ntai, K.L.T. Tran, K.J. Weaver, D.C. Forbes, J.H. Davis, Novel Brønsted acidic ionic liquids and their use as dual solvent–catalysts, *J. Am. Chem. Soc.* 124(21) (2002) 5962-5963.
- [33] T. Welton, Room-temperature ionic liquids. Solvents for synthesis and catalysis, *Chem. Rev.* 99(8) (1999) 2071-2084.
- [34] L.A. Blanchard, D. Hancu, E.J. Beckman, J.F. Brennecke, Green processing using ionic liquids and CO<sub>2</sub>, *Nature* 399(6731) (1999) 28-29.
- [35] Y. Nonomura, S. Komura, K. Tsujii, Adsorption of disk-shaped Janus beads at liquid–liquid interfaces, *Langmuir* 20(26) (2004) 11821-11823.
- [36] R. Aveyard, B.P. Binks, J.H. Clint, Emulsions stabilised solely by colloidal particles, *Adv. Colloid Interface Sci.* 100–102 (2003) 503-546.
- [37] J. Frelichowska, M.-A. Bolzinger, Y. Chevalier, Effects of solid particle content on properties of o/w Pickering emulsions, *J. Colloid Interface Sci.* 351(2) (2010) 348-356.
- [38] F. Yang, Q. Niu, Q. Lan, D. Sun, Effect of dispersion pH on the formation and stability of Pickering emulsions stabilized by layered double hydroxides particles, *J. Colloid Interface Sci.* 306(2) (2007) 285-295.
- [39] J. Yang, S. Aschemeyer, H.P. Martinez, W.C. Trogler, Hollow silica nanospheres containing a silafluorene-fluorene conjugated polymer for aqueous TNT and RDX detection, *Chem. Commun.* 46(36) (2010) 6804-6806.
- [40] F. Liang, K. Shen, X. Qu, C. Zhang, Q. Wang, J. Li, J. Liu, Z. Yang, Inorganic Janus nanosheets, *Angew. Chem. Int. Ed.* 50(10) (2011) 2379-2382.
- [41] A. Perazzo, V. Preziosi, S. Guido, Phase inversion emulsification: Current understanding and applications, *Adv. Colloid Interface Sci.* 222 (2015) 581-599.
- [42] Y. Leng, J. Wang, D. Zhu, X. Ren, H. Ge, L. Shen, Heteropolyanion-based ionic liquids: Reaction-induced self-separation catalysts for esterification, *Angew. Chem. Int. Ed.* 48(1) (2009) 168-171.
- [43] P. Gouzerh, A. Proust, Main-group element, organic, and organometallic derivatives of polyoxometalates, *Chem. Rev.* 98(1) (1998) 77-112.

- 
- [44] J. Li, Y. Zhou, D. Mao, G. Chen, X. Wang, X. Yang, M. Wang, L. Peng, J. Wang, Heteropolyanion-based ionic liquid-functionalized mesoporous copolymer catalyst for Friedel–Crafts benzylation of arenes with benzyl alcohol, *Chem. Eng. J.* 254 (2014) 54-62.
- [45] J. Tang, P.J. Quinlan, K.C. Tam, Stimuli-responsive Pickering emulsions: Recent advances and potential applications, *Soft Matter* 11(18) (2015) 3512-3529.
- [46] R. Guterman, M. Ambrogi, J. Yuan, Harnessing poly(ionic liquid)s for sensing applications, *Macromol. Rapid Commun.* 37 (2016) 1106-1115.